

COMMUNICATION

Slippery Nanoemulsion-Infused Porous Surfaces (SNIPS): Anti-Fouling Coatings that Can Host and Sustain the Release of Water-Soluble Agents

Received 00th January 20xx,
Accepted 00th January 20xx

DOI: 10.1039/x0xx00000x

Harshit Agarwal,¹ Thomas J. Polaske,² Gabriel Sánchez-Velázquez,¹ Helen E. Blackwell,² and David M. Lynn^{1,2,*}

We report the design of ‘slippery’ nanoemulsion-infused porous surfaces (SNIPS). These materials are strongly antifouling to a broad range of substances, including microorganisms. Infusion with water-in-oil nanoemulsions also endows these slippery coatings with the ability to host and sustain the release of water-soluble agents, including polymers, peptides, and nucleic acids, opening the door to new applications of liquid-infused materials.

The fouling of surfaces by liquids, microorganisms, and other substances has a wide range of economic and environmental consequences.^{1, 2} Many approaches have been developed to design anti-fouling surfaces, including chemical modifications using fluorinated compounds, structural modifications to introduce combinations of micro/nano-porosity and texture, and incorporation of active or passive controlled release strategies.³⁻⁷ These materials have shown promise on short time scales and in well-defined environments, but ultimately fail when deployed in the field or for extended periods.

Slippery liquid-infused porous surfaces (SLIPS) and lubricant-impregnated surfaces (LIS) represent an emerging class of synthetic soft material coatings that exhibit robust and unique anti-fouling behaviours, many of which stem from the presence of a mobile surface layer of lubricating fluid that allows substances to simply slide or roll off.⁸⁻¹⁴ In the decade since their introduction in 2011, SLIPS and LIS have become a substantial focus of research on anti-fouling and smart-wetting materials,¹³⁻¹⁵ and designs of these materials have been commercialized to aid the dispensing of liquids and prevent fouling in aqueous, biological, and marine environments. The development of new approaches to the fabrication of SLIPS and LIS that improve stability and introduce new functions or behaviours will continue to expand practical utility and open the door to new applications for liquid-infused materials.

The first examples of SLIPS involved infusion of perfluorinated lubricating liquids into nanoporous polytetrafluoroethylene (PTFE) membranes.⁹ Since that report, many approaches have expanded the combinations of porous/textured surfaces and lubricating liquids that can be used as building blocks for the assembly of SLIPS.¹³⁻¹⁵ Most of this past work has focused on designing SLIPS that can repel, attract, or manipulate materials or substances with which they come into direct contact.¹³⁻¹⁶ For example, many SLIPS can reduce or prevent microbial colonization or reduce thrombosis on the surfaces of medical devices.^{11, 17} Most of these materials can do little, however, to influence behaviours or events that occur in surrounding environments that do not come into direct contact with the liquid interface (e.g., to kill non-adherent bacteria or prevent thrombus formation in surrounding areas).

One approach to designing ‘multifunctional’ SLIPS that can also affect changes in surrounding media is to design liquid-infused surfaces that contain active agents that can be released into surrounding environments. Despite the conceptual simplicity of this approach, incorporation of controlled release strategies into SLIPS has been challenging due to constraints imposed by the chemical nature of the porous matrix and the infused liquid phases, and only a few recent studies have reported the design of ‘controlled release’ SLIPS. We previously reported a strategy for the loading and release of triclosan, a broad-spectrum antimicrobial agent, into polymer-based SLIPS.¹⁸ That approach led to SLIPS that could kill planktonic microbial pathogens in solution and exhibit improved anti-biofouling properties. The behaviours of those films were understood to arise from the solubility of triclosan (a hydrophobic molecule) in an infused silicone oil phase, which facilitated gradual partitioning from the polymer matrix to the surrounding aqueous phase. In another example, Guodie et al. reported the release of nitric oxide from silicone oil-infused rubber tubing by impregnating tubing with a nitric oxide donor prior to infusion with oil.¹⁹ These approaches are useful and provide important examples of ways in which the infused oil phase and/or underlying matrix can be used as depots to host and release active agents. They are inherently

¹Dept. of Chemical & Biological Engineering, University of Wisconsin-Madison, 1415 Engineering Dr., Madison, WI 53706, USA

²Dept. of Chemistry, University of Wisconsin-Madison, 1101 University Ave., Madison, WI 53706, USA

Electronic Supplementary Information (ESI) available: Materials and methods and additional plots, tables, and images showing characterization of slippery surfaces. See DOI: 10.1039/x0xx00000x

limited, however, to hosting and releasing *hydrophobic* agents because of constraints imposed by the nature of the hydrophobic matrices and infused oils typically used to design SLIPS. The design of SLIPS that enable the loading and release of *hydrophilic* agents would open the door to new applications, but creates an interesting set of design challenges.

The work reported here addresses challenges related to the release of water-soluble agents from liquid-infused materials by adopting design strategies that involve infusion with water-in-oil (w/o) nanoemulsions (instead of conventional oils) as the hydrophobic liquid lubricant phase. We hypothesized that if w/o nanoemulsions could be infused into porous surfaces without loss of slippery character, the fugitive water droplets in these liquids could be used to store and promote the release of water-soluble agents.

We began our studies using (i) commercially available porous PTFE membranes similar to those used for the infusion of conventional oils to design SLIPS,^{9, 20} and (ii) nanoemulsion formulations reported to lead to thermodynamically stable w/o nanoemulsions in past studies.²¹⁻²⁴ We reasoned that these nanoemulsion formulations would provide an overall hydrophobic interface upon infusion into PTFE membranes, owing to their majority oil phase, but that the water droplets within them would be sufficiently small to allow uniform distribution into the microscale pores (Fig S1) of PTFE membranes without sedimenting or creaming. A general schematic illustrating the overall structure of 'SNIPS' designed using this approach is shown in Fig 1A.

A series of initial experiments demonstrated that PTFE membranes could be infused with model w/o nanoemulsions

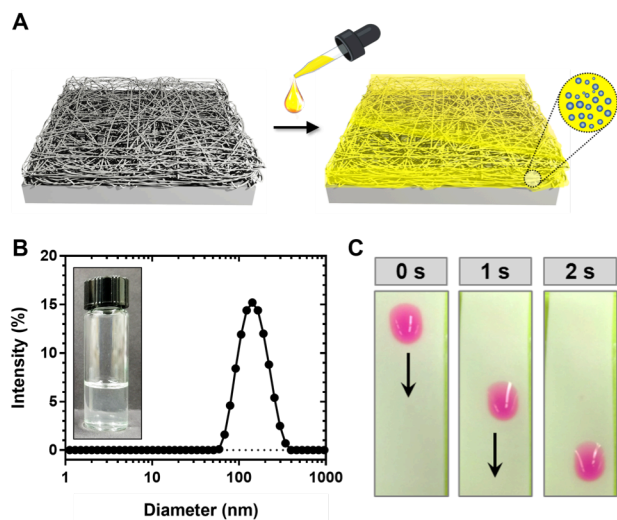


Figure 1. (A) Schematic of a slippery nanoemulsion-infused porous surface (SNIPS) formed by infusion of w/o nanoemulsion (yellow) into a porous PTFE membrane (gray). The inset shows an enlarged view of the structure of the nanoemulsion, containing small nanoscale water droplets (blue) dispersed in a continuous oil phase (yellow). (B) Plot showing the intensity-weighted particle size distribution of a w/o nanoemulsion; a unimodal distribution is shown with a z-average size of 134 nm and a PDI of 0.134. The inset shows a digital picture of a w/o nanoemulsion in a sample vial. (C) Digital pictures, acquired from a top-down perspective, of a 25- μ L water droplet (coloured pink to ease visual inspections) sliding on a SNIPS tilted at 30°.

to produce SNIPS that were both slippery and stable upon contact with other substances. For all experiments below, we used water/hexadecane nanoemulsions prepared using previously reported phase inversion methods (see Methods in SI).²¹⁻²⁴ Fig 1B shows an image of an optically clear nanoemulsion and a droplet size distribution ($D_z = 34$ nm; PDI = 0.134). Samples of nanoemulsion placed onto PTFE membranes (avg pore size = 5 μ m; see Fig S1 for SEM images) readily spread ($\theta \approx 0^\circ$) and infused into the membrane, as evident from changes in the visual appearance of these surfaces from rough and opaque to translucent after infusion.

Fig 1C shows top-down views of a 25 μ L droplet of water placed on a SNIPS sample tilted at an angle of $\sim 30^\circ$; the droplet slid over a length of 4 cm in ~ 2 s (droplets did not slide on non-infused membranes under these conditions). This high degree of mobility is consistent with (i) behaviours of water droplets on conventional oil-infused SLIPS and (ii) the presence of a 'slippery' nanoemulsion-based lubricant phase on the surface that remains stable in the presence of water droplets ($S_{os(w)} \geq 0$; see Table S1).^{9, 12, 14} These results also demonstrate

Table 1: Sliding Speeds of Complex Liquids on SNIPS

Liquids	Sliding Time [‡] (s)
Milk	1.3 \pm 0.6
Blood	1.7 \pm 0.5
Urine	1.3 \pm 0.6
Lake Water	1.3 \pm 0.6
Soy Sauce	1.7 \pm 0.4

[‡] Values are the mean and standard error of four independent replicates. Experiments were performed by placing droplets of liquids (25 μ L) on SNIPS held at angles of 30° and measuring sliding times over a fixed distance (see Methods for details).

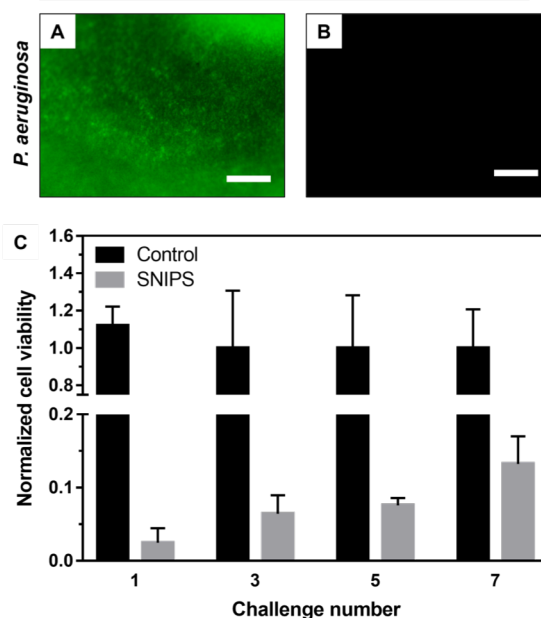


Figure 2. A,B) Fluorescence microscopy images showing (A) control and (B) SNIPS surfaces after incubation in suspensions of *P. aeruginosa* for 24 h. Scale bars = 400 μ m. (C) Plot showing the viability of *S. aureus* cells associated with the surfaces of control PTFE membranes (black bars) and SNIPS (gray bars) after each of seven consecutive 24 h challenges in *S. aureus* inoculum (see main text and Supporting Information for details).

that the presence of the fugitive water phase does not substantially impact slippery character.

These SNIPS are slippery, stable, and substantially non-fouling when placed in repeated contact with a broad range of other chemically complex liquids, including milk, whole blood, human urine, lake water, and soy sauce (Table 1). They are also able to strongly resist attachment and subsequent biofouling by common bacterial pathogens, including both Gram-negative (*E. coli*, *P. aeruginosa*) and Gram-positive (*S. aureus*) bacteria, upon incubation in bacterial cultures for 24 h at 37 °C (see Fig 2A-B and Fig S2). To characterize anti-biofouling performance over extended periods and under more challenging conditions, we also performed experiments in which SNIPS were repeatedly immersed and incubated in cultures of *S. aureus* for 24 h and then, after each 24 h challenge, removed and characterized to quantify biofouling (see Methods in Supporting Information). Figure 2C shows results of an experiment involving seven consecutive 24 h bacterial challenges, and reveals SNIPS to maintain their robust anti-biofouling properties, relative to bare PTFE controls, for up to seven challenges (fluorescence microscopy images of the surfaces of control and SNIPS surfaces after the seventh challenge are shown in Figure S2).

To further characterize the structures and properties of SNIPS and determine the feasibility of using the infused nanoemulsions as platforms to host and release water-soluble cargo, we prepared SNIPS using nanoemulsions loaded with FITC-dextran, a water-soluble polymer used widely as a model for the loading and release of macromolecules in drug delivery systems. Nanoemulsions prepared with FITC-dextran were similar to those described above using water ($D_z = 124$ nm; see Fig S3). Characterization of SNIPS fabricated using FITC-dextran-loaded nanoemulsions by fluorescence (Fig 3A) and confocal fluorescence (Fig 3C) microscopy revealed uniform green fluorescence distributed over (3A) and throughout the thickness (~ 200 μm (Figure S1B); 3C) of the PTFE membranes. Taken together, these results suggest that nanoemulsions are able to infuse into and spread uniformly within the porous structures of these membranes without the aqueous droplets carrying the FITC-dextran being filtered out by size exclusion.

FITC-loaded SNIPS released FITC-dextran into surrounding aqueous media for at least 90 d when incubated in PBS at 37 °C. Fig 3D shows the cumulative amount of FITC-dextran released over time for a representative set of SNIPS samples. These results reveal $\sim 38\%$ of the total loaded FITC-dextran was released over the first 24 h, followed by the gradual release of an additional $\sim 40\%$ over the remainder of this 3-month experiment. This increase in fluorescence in solution was accompanied by a corresponding gradual decrease in the fluorescence of the SNIPS themselves (as revealed by fluorescence microscopy; Fig 3B shows a sample after 85 d; see Fig S4 for images acquired at other points). Results shown in Fig 3D reveal $\sim 80\%$ of the total loaded FITC-dextran was released over 90 d; we did not characterize release for longer time periods as part of this current study.

The release profile in Fig 3D exhibits an initial burst release phase, followed by a slower and more sustained phase that is

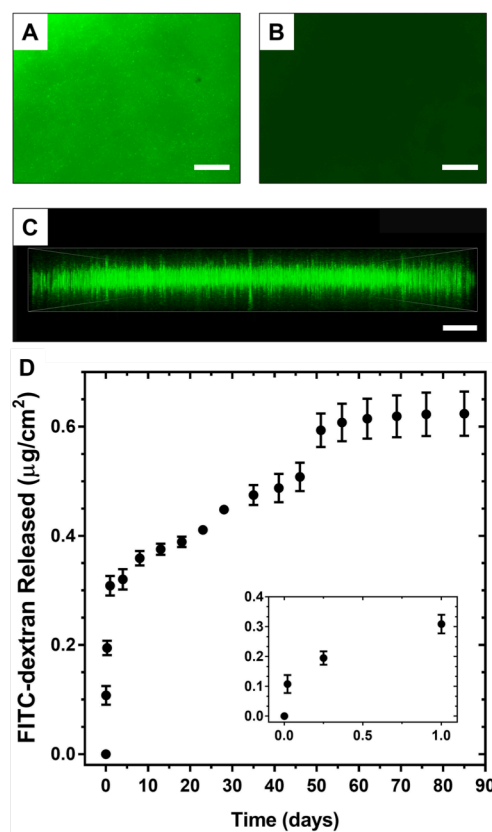


Figure 3. (A,B) Top-down fluorescence microscopy images showing FITC-dextran-loaded SNIPS (A) before and (B) after ($t = 85$ d) incubation in PBS at 37 °C. Scales bars are 400 μm ; see also Fig S4. (C) Confocal microscopy image showing combined z-stack of FITC-dextran-loaded SNIPS. The image shows the x-z plane; the scale bar is 200 μm . (D) Plot showing amount of FITC-dextran released from FITC-dextran-loaded SNIPS incubated in PBS at 37 °C. Total loading = 0.79 ± 0.04 $\mu\text{g}/\text{cm}^2$ (see Methods in Supporting Information). Data points represent the mean of four replicates and error bars are standard error. Inset shows release over the first day of incubation.

approximately linear over 50 d. The initial burst of release occurs upon the initial wetting of a thin layer of nanoemulsion at the SNIPS surface and could result, at least in part, from the loss of some non-entrained or excess nanoemulsion. We note, however, that samples of FITC-dextran-loaded SLIPS remained slippery (as determined by measurements of droplet sliding times and by additional anti-biofouling assays discussed below) after initial immersion and over the entire 90-d period of this experiment. It is also possible that this initial phase could arise from the accumulation of FITC-dextran at the top surface of the membrane during infusion, although we did not observe evidence of a gradient in the distribution of FITC in the confocal image in Fig 3C.

After this initial release phase, we observed approximately linear (zero-order) release, suggestive of a steady-state diffusion regime. This is consistent with a mechanism that involves the diffusion of aqueous droplets containing FITC-dextran through the barrier oil phase and subsequent partitioning and coalescing with the surrounding aqueous phase. Because FITC-dextran is not soluble in hexadecane, we consider it unlikely that FITC-dextran is released through a

mechanism that involves partitioning into and/or diffusion through the bulk oil phase, as reported previously for other controlled release SLIPS loaded with hydrophobic small molecules.^{18, 19, 25} We note that, overall, there are likely other factors that influence the rate of release of FITC-dextran into the aqueous phase, including (i) size-dependent segregation of the fugitive aqueous phase droplets within the pores of the PTFE membranes (due to the nanometer-scale sizes of these water droplets, characterization of size distribution of the water droplets in infused samples by confocal microscopy was not feasible), and (ii) changes in the size distribution of aqueous droplets in the infused nanoemulsion phase over time resulting from destabilization mechanisms such as gravitational separation, coalescence, and Ostwald ripening (see Fig S5 for characterization of changes in the z-average droplet sizes of nanoemulsions, with and without FITC, as a function of time incubated at 37 °C). As noted above, these FITC-loaded SNIPS remained slippery to aqueous droplets and anti-fouling to bacteria for the duration of these experiments (reducing biofouling by ~80% compared to controls after 85 d; see Fig S6) suggesting that the release of FITC-dextran did not result from the gradual and continuous loss of bulk nanoemulsion from these materials.

The results above demonstrate that nanoemulsions can be used to design slippery, anti-fouling materials that can host and sustain the subsequent release of a model water-soluble polymer that is not soluble in the types of hydrophobic bulk oil phases that are typically used to design conventional SLIPS and LIS. This SNIPS approach thus creates opportunities to design liquid-infused materials that have the ability to slowly release or administer a broad range of hydrophilic active agents that have the capacity to either (i) further improve the anti-fouling properties of these materials or (ii) impart a range of other functions and behaviours that are not possible using conventional liquid-infused materials. In this context, we note that the approach reported here is modular, and can likely be extended to the encapsulation, infusion, and release of a broad range of other hydrophilic agents. The results of additional experiments shown in Fig S7 reveal that it is possible to design SNIPS loaded with peptides, proteins, nucleic acids, and water-soluble small-molecules using the model nanoemulsion formulations and procedures reported above. We also note that release rates will likely depend on the physical and chemical properties of the infused nanoemulsion, the underlying matrix, and the physicochemical properties of the loaded agents. Additional studies exploring the properties and behaviours of these and other related SNIPS systems are currently underway and will be reported in due course.

In summary, we have reported the design of slippery nanoemulsion-infused porous surfaces (SNIPS) that remain slippery and anti-fouling in contact with a broad range of liquids and organisms, including several types of bacterial pathogens. Our results show that SNIPS can host and sustain the release of water-soluble cargo for at least 90 d while retaining anti-fouling character. Moreover, this nanoemulsion-based approach is modular, and can be used to design SNIPS hosting a range of other water-soluble agents, including

peptides, proteins, and nucleic acid constructs. We anticipate that this approach will thus prove useful in the design of inherently anti-fouling and multifunctional liquid-infused surfaces that can affect new and useful levels of control over events and behaviours in their surrounding environments.

Financial support was provided by the NSF through a grant provided to the UW–Madison Materials Research Science and Engineering Center (MRSEC; DMR-1720415) and by the UW–Madison Wisconsin Alumni Research Foundation (WARF) through the WARF Accelerator Program and the Draper Technology Innovation Fund. Bacterial assay development was supported by the NIH (R35 GM131817 to H.E.B.). T.J.P. was supported in part by the UW–Madison NIH Chemistry–Biology Interface Training Program (T32 GM008505).

Notes and references

1. *Marine and Industrial Biofouling*, Springer, 1 edn., **2009**.
2. *The Role of Biofilms in Device-Related Infections*, Springer, 1 edn., **2009**.
3. M. Liu, S. Wang and L. Jiang, *Nat. Rev. Materials*, 2017, **2**, 17036.
4. A. Tuteja, W. Choi, M. Ma, J. M. Mabry, S. A. Mazzella, G. C. Rutledge, G. H. McKinley and R. E. Cohen, *Science*, 2007, **318**, 1618.
5. I. Banerjee, R. C. Pangule and R. S. Kane, *Adv. Mater.*, 2011, **23**, 690.
6. Z. Chu and S. Seeger, *Chem. Soc. Rev.*, 2014, **43**, 2784–2798.
7. Z. K. Zander and M. L. Becker, *ACS Macro Lett.*, 2018, **7**, 16–25.
8. A. Lafuma and D. Quéré, *EPL (Europhysics Letters)*, 2011, **96**, 56001.
9. T.-S. Wong, S. H. Kang, S. K. Y. Tang, E. J. Smythe, B. D. Hatton, A. Grinthal and J. Aizenberg, *Nature*, 2011, **477**, 443–447.
10. S. Anand, A. T. Paxson, R. Dhiman, J. D. Smith and K. K. Varanasi, *ACS Nano*, 2012, **6**, 10122–10129.
11. P. Kim, T.-S. Wong, J. Alvarenga, M. J. Kreder, W. E. Adorno-Martinez and J. Aizenberg, *ACS Nano*, 2012, **6**, 6569–6577.
12. B. R. Solomon, S. B. Subramanyam, T. A. Farnham, K. S. Khalil, S. Anand and K. K. Varanasi, in *Non-wettable Surfaces: Theory, Preparation and Applications*, The Royal Society of Chemistry, 2017, DOI: 10.1039/9781782623953-00285, pp. 285–318.
13. J. Li, E. Ueda, D. Paulssen and P. A. Levkin, *Adv. Funct. Mater.*, 2019, **29**, 1802317.
14. M. Villegas, Y. Zhang, N. Abu Jarad, L. Soleymani and T. F. Didar, *ACS Nano*, 2019, **13**, 8517–8536.
15. S. Peppou-Chapman, J. K. Hong, A. Waterhouse and C. Neto, *Chem. Soc. Rev.*, 2020, **49**, 3688–3715.
16. D. P. Regan and C. Howell, *Curr. Opin. Colloid Interface Sci.*, 2019, **39**, 137–147.
17. I. Sotiri, J. C. Overton, A. Waterhouse and C. Howell, *Exp. Biol. Med.*, 2016, **241**, 909–918.
18. U. Manna, N. Raman, M. A. Welsh, Y. M. Zayas-Gonzalez, H. E. Blackwell, S. P. Palecek and D. M. Lynn, *Adv. Funct. Mater.*, 2016, **26**, 3599–3611.
19. M. J. Goudie, J. Pant and H. Handa, *Sci. Rep.*, 2017, **7**, 13623.
20. A. K. Epstein, T.-S. Wong, R. A. Belisle, E. M. Boggs and J. Aizenberg, *Proc. Natl. Acad. Sci. U. S. A.*, 2012, **109**, 13182–13187.
21. H. Wu, C. Ramachandran, N. D. Weiner and B. J. Roessler, *Int. J. Pharm.*, 2001, **220**, 63–75.
22. M. Porras, C. Solans, C. González and J. M. Gutiérrez, *Colloids Surf. Physicochem. Eng. Aspects*, 2008, **324**, 181–188.
23. L.-C. Peng, C.-H. Liu, C.-C. Kwan and K.-F. Huang, *Colloids Surf. Physicochem. Eng. Aspects*, 2010, **370**, 136–142.
24. A. Gupta, H. B. Eral, T. A. Hatton and P. S. Doyle, *Soft Matter*, 2016, **12**, 2826–2841.
25. M. J. Kratochvil, M. A. Welsh, U. Manna, B. J. Ortiz, H. E. Blackwell and D. M. Lynn, *ACS Infect. Dis.*, 2016, **2**, 509–517.